

## Thermochemical Behaviour of Red Algae: Kinetics and Mechanism of the Pyrolysis

Hassan Bouaik<sup>1</sup>, A. Tabal<sup>1</sup>, A. Aboulkas<sup>1,2\*</sup>, K. El Harfi<sup>1,2</sup>

<sup>1,2</sup>Laboratoire Interdisciplinaire de Recherche en Sciences et Techniques, Faculté Polydisciplinaire de Béni-Mellal, Université Sultan Moulay Slimane, BP 592, 23000 Béni-Mellal, Maroc.

Corresponding author: Hassan Bouaik

**Abstract:** The present work assesses a possible process for treating red algal in an environmentally friendly way. It is based on the pyrolysis of these algal for energetic valorization to evaluate its bioenergy potential. The pyrolytic and kinetic characteristics of red algal as a model for algal biomass were evaluated and compared at heating rates of 5, 10, 20 and 50 °C min<sup>-1</sup> from 0 to 900 °C in an inert atmosphere. The DTG curves showed three distinct stages of degradation; dehydration, devolatilization, and residual decomposition. The kinetic analysis was established by the isoconversional methods of Friedman (FR), Flynn-Wall-Ozawa (FWO), and Vyazovkin (VYA) methods) to estimate activation energy, the master-plot methods were introduced to establish kinetic models. Activation energy values were shown to be 227 ± 8, 214 ± 2 and 224,2 ± 3 kJ mol<sup>-1</sup> as calculated by FR, FWO, and VYA methods, respectively. The devolatilization stage of red algal could be described by the Third-order equation (n = 3). It is shown that the isoconversional kinetic methods provide reliable kinetic information suitable for adequately choosing the kinetic model which best describes the thermal decomposition of red algal. The composite differential method was used to obtain the following kinetic triplet:  $g(x) = [(1-x)^{-2} - 1]/2$ ,  $E_a = 221,6 \text{ kJ/mol}$ ,  $R = 0.99$ .

**Keywords:** red Algal; thermal degradation; Isoconversional methods; master-plots method; Kinetic triplet.

### 1. Introduction

The limited reserve of fossil fuels and the increase in energy consumption compels us to look for alternative and renewable sources of energy. Energy demand and climate change have led the world to discover new sources of renewable, secure, environmentally friendly, affordable and above all sustainable energy [1]. Due to its abundance, renewability and higher energy density, biomass is considered as the most promising alternative-energy source to fuel the future of mankind [2]. Macroalgae is a source of aquatic biomass and potentially represents an important source of renewable energy in the coming years. The average photosynthetic efficiency of aquatic biomass is 6 to 8% [3]. As a result, there is interest in alternative biomass resources, including the biomass of an aquatic environment which is much higher than those of terrestrial biomass (1.8-2.2%).

The marine areas of Morocco include almost 3500 km of coastline [4]. The macroalgae are considered economically valuable resources due to their ability to produce high yields of commercially valuable biomass [5]. The abundance of the *Gelidium sesquipedalian* macroalgae encouraged the development of the industrial units specialized in the production of the agar-agar, whose Morocco is the third producer in the world [6]. The *Gelidium*

represents 90% of the harvest of the marine algae treated locally and that generates an important quantity of waste that cannot be treated very well [7]. The valorization of red macroalgae by new technologies of thermochemical conversion, and more particularly of pyrolysis, seems to be particularly interesting. During pyrolysis, a significant amount of biofuel (biofuel, biofuel, and biogas) is produced [8]. These red macroalgae can be used as biofuel. Also, pyrolytic gas was used as fuel, while coal has various applications, including fertilizers, activated carbon. And the biochar can be used as a soil amendment [9].

Thermogravimetric analysis (TGA) has been selected for the thermal decomposition process [10]. The kinetic data obtained from the TGA is very useful to help understand the processes and mechanisms of thermal degradation. These data can also be used as model input parameters for thermal degradation reaction [11]. Numerous studies have been published on the characteristics and kinetics of the pyrolysis of macroalgae [12]. Conducted a behavioral study by pyrolysis of the main carbohydrates of brown macroalgae and Py-GC / MS results. The methods, FR, FWO, and KAS were adopted to determine the kinetic parameters of the reaction. The macroalgae red species *Gelidium* presented the reaction mechanism of the random

nucleation followed by a reaction-order model ( $n = 3$ ). The activation energy calculated by these three methods is similar. However, there are no reports in the literature on the kinetics and mechanism of pyrolysis of red algae.

Red algae represent abundant biomass at low cost for bioenergy production, but its thermal conversion to energy requires an understanding of its pyrolytic characteristics and kinetics. This study focused on the thermal characterization of this biomass at low cost, using thermogravimetric analysis. Kinetic parameters were determined by isoconversional conversion and differential methods) and the kinetic model was determined by the integral master plots and differential methods. Finally, to verify the accuracy of the determined reaction model data ( $f(\alpha)$ ), the direct differential method was applied.

## 2. Experimental

### 2.1 Materials and samples preparation

Red algal used in this study as a feedstock was obtained from the industrial processing of red macroalgae to obtain Agar product (SETEXAM company, Kenitra-Morocco). Before use, algal waste was air-dried, ground, and sieved to obtain particles in the ranges of 0.1-0.2 mm. The chemical compositions of samples are depicted in Table 1.

**Table 1.** Main characteristics of red algal[13].

Proximate analysis (wt.%)	Moisture	8,45
	Volatile matter	70,60
	Ash	10,85
Ultimate analysis (wt.%)	Fixed carbon	18,55
	C	26,67
	H	3,84
	N	2,90
	S	0,89
	O	54,85
HHV (MJ/kg) Atomic		15,18
	H/C	1,73
	O/C	1,54
Empirical formula	CH <sub>1,73</sub> O <sub>1,54</sub> N <sub>0,093</sub>	

### 2.2 Experimental Techniques

Red algae samples were subjected to thermogravimetric analysis (TGA) in an inert atmosphere of nitrogen. Rheometric Scientific STA 1500 TGA analyzer was used to measure and record the sample mass change with temperature for the pyrolysis reaction. Thermogravimetric curves were obtained at four different heating rates (5, 10, 20, and 50 K min<sup>-1</sup>) between 25C° and 900 C°. Nitrogen gas was used as an inert purge gas to displace air in the pyrolysis zone, thus avoiding unwanted oxidation of the sample. A flow rate of around 60 ml min<sup>-1</sup> was fed to the system from a point below the sample and purge time of 60 min (to be sure the air was eliminated from the system and the atmosphere

is inert). The balance can hold a maximum of 45 mg; therefore, all sample amounts used in this study averaged approximately 20 mg. The reproducibility of the experiments is acceptable and the experimental data presented in this paper corresponding to the different operating conditions are the mean values of runs carried out two or three times.

### 2.3 Kinetic modeling

General kinetic equation of heterogeneous solid-state thermal transformation at a linear temperature heating rate has been traditionally described as, [14]: (1) model-free kinetics to allow for a change in mechanism during a reaction, and (2) mass transfer limitations are reduced by the use of multiple heating rates. In contrast, model kinetic methods generally involve a single heating rate, which is disadvantageous because the activation energy varies with the heating rate due to mass/energy transfer effects. The conversion of biomass can be calculated as:

$$x = \frac{w_0 - w_t}{w_0 - w_\infty} \quad (1)$$

Where  $w$  is the mass of the sample at a given time  $t$  and  $w_0$  and  $w_\infty$  refer to values at the beginning and the end of the mass loss event of interest. The rate of heterogeneous solid-state reactions can be generally described by

$$\frac{dx}{dt} = K(T)f(x) \quad (2)$$

$K(T)$  is a temperature-dependent constant and  $f(x)$  is the reaction model, which describes the dependence of the reaction rate on the extent of reaction.

$K(T)$  the temperature dependence of the rate of weight loss, is often modeled successfully by the Arrhenius equation,

$$K(T) = A \cdot \exp\left(-\frac{E}{RT}\right) \quad (3)$$

Where  $E$ : is the activation energy,  $A$ : the pre-exponential factor, and  $R$ : the gas constant.

The mathematical description of the data for a single-step solid-state decomposition is usually defined in terms of a kinetic triplet: the activation energy,  $E$ ; the Arrhenius parameter,  $A$ ; and an algebraic expression of the kinetic model as a function of the fractional conversion  $x$ ,  $f(x)$ . These terms can be related to experimental data as follows. By combining the Eq (1) and (3), the reaction rate can be written in the form:

$$\frac{dx}{dt} = A \cdot \exp\left(-\frac{E}{RT}\right) f(x) \quad (4)$$

#### 2.3.1 Friedman method.

This method is a differential isoconversional method, and it directly based on Eq (4) whose logarithm is[15].

$$\ln\left(\frac{dx}{dt}\right) = \ln\left(\beta \frac{dx}{dt}\right) = \ln[A \cdot f(x)] - \frac{E}{RT} \quad (5)$$

From this equation, it is easy to obtain values for  $E$  over a wide range of conversions by plotting  $\left(\frac{dx}{dt}\right)$  against  $1/T$  for a constant  $x$  value.

#### 2.3.2 Flynn–Wall–Ozawa method (FWO).

The above rate expression can be transformed into non-isothermal rate expressions describing reaction rates as a function of temperature at a constant  $\beta$  ( $\beta = dT/dt$ ):

The standard Eq. (4) can be shown as follows:[16] ; [17]

$$\frac{dx}{dT} = \frac{A}{\beta} \cdot \exp\left(-\frac{E}{RT}\right) f(x) \quad (6)$$

Integrating up to the conversion, a, Eq. (6) gives

$$\int_0^x \frac{dx}{f(x)} = g(x) = \frac{A}{\beta} \int_{T_0}^T \exp\left(-\frac{E}{RT}\right) dT \quad (7)$$

Where g(x) is the integral kinetic function or integral reaction model when its form is mathematically defined.

One of the methods to obtain the E from dynamic data may be the one used by Flynn, Wall, and Ozawa [18], using Doyle's approximation of p(x) [19], which involves measuring the temperatures corresponding to fixed values of x from experiments at different heating rates. This is one of the integral methods that can determine the E which does not require the knowledge of reaction order.

$$\ln(\beta) = \ln\left(\frac{AE}{Rg(x)}\right) - 5,331 - 1,052 \frac{E}{RT} \quad (8)$$

Thus, for x = const. The plot ln(β) versus 1 /T, obtained from curves recorded at several heating rates, should be a straight line whose slope can be used to evaluate the activation energy.

### 2.3.3 Integral isoconversional method: Vyazovkin (VYA)

Vyazovkin and Lesnikovick developed another isoconversional method allowing evaluation of simple and complex reactions [20].

In Eq. (7), since E/2RT >> 1, the temperature integral can be approximated by

$$\int_{T_0}^T \exp\left(-\frac{E}{RT}\right) dT \approx \frac{R}{E} T^2 \exp\left(-\frac{E}{RT}\right) \quad (9)$$

By replacing the temperature integral and taking the logarithm, we obtain this result.

$$\ln\left(\frac{\beta}{T^2}\right) = \ln\left(\frac{RA}{Eg(x)}\right) - \frac{E}{RT} \quad (10)$$

For each conversion value (x), the plot of ln (β/T<sup>2</sup>) as a function 1/T, gives a straight line with slope E/R. Thus, the activation energy is obtained at every degree of conversion x.

### 2.3.4 Pre-exponential factor and reaction mechanism.

Model-free methods can be used to study the Ea values and to find out their dependency on the conversion

(x). As the kinetic parameters are computed without knowing the reaction mechanism, using iso-conversional methods is not suggested to evaluate the pre-exponential factor. There are several approaches to predict the reaction mechanism and pre-exponential factor and some of them are explained in [21], [22]. In the present study two different approaches, i.e. master plots and kinetic compensation effect (KCE), were used to evaluate the reaction mechanism.

### 2.3.5 Integral master plots

Using as a reference point at x =0.5, the following differential master equation is easily derived from Eq. (5):

$$\frac{f(x)}{f(0,5)} = \frac{dx/dt}{(dx/dt)_{0,5}} \frac{\exp(E/RT)}{\exp(E/RT_{0,5})} \quad (11)$$

Where(dx/dt)<sub>0,5</sub>, T<sub>0,5</sub> and f (0.5) are respectively the reaction rate, the temperature reaction and the differential conversion function at x=0.5. The theoretical curves are obtained by plotting  $\frac{f(x)}{f(0,5)}$  against x for different reaction models. The resulting experimental

$\frac{dx/dt}{(dx/dt)_{0,5}} \frac{\exp(E/RT)}{\exp(E/RT_{0,5})}$  values are plotted against x and matched with the theoretical masterplots[20], [23].

Using as reference point at x =0.5, the following integral master equation is easily derived from Eq. (7):

$$\frac{g(x)}{g(0,5)} = \frac{P(x)}{P(x_{0,5})} \quad (12)$$

where P(x<sub>0,5</sub>)is the temperature integral at x = 0.5 P(x) has been obtained according to the Senum-Yang approximation[24].

$$p(x) = \frac{e^{-x}}{x} \frac{x^3+18x^2+86x+96}{x^4+20x^3+120x^2+240x+120} \quad (13)$$

Using the Coats–Redfern approximation (Eq. (10) the Eq. (12) becomes:

$$\frac{g(x)}{g(0,5)} = \frac{\exp(-E/RT)T^2}{\exp(-E/RT_{0,5})T_{0,5}^2} \quad (14)$$

The theoretical curves are obtained by plotting  $\frac{g(x)}{g(0,5)}$  against x for different reaction models. The resulting experimental  $\frac{T^2}{T_{0,5}^2} \frac{\exp(-E/RT)}{\exp(-E/RT_{0,5})}$  values are plotted against x and matched with the theoretical masterplots [25].

**Table 2.** Set of reaction models applied to describe the reaction kinetics in heterogeneous solid-state systems[20], [23], [25].

Model	symbol	Differential form	
		$f(x) = \frac{1}{K} \left(\frac{dx}{dt}\right)$	Integral form g(x)=kt
Nucleation models			
Power law	P2	$2 x^{1/2}$	$x^{1/2}$
Power law	P3	$3 x^{2/3}$	$x^{1/3}$
Power law	P4	$4 x^{3/4}$	$x^{1/4}$
Avarami-Erofeyev	A2	$2(1-x)[-ln(1-x)]^{1/2}$	$[-ln(1-x)]^{1/2}$
Avarami-Erofeyev	A3	$3(1-x)[-ln(1-x)]^{2/3}$	$[-ln(1-x)]^{1/3}$
Avarami-Erofeyev	A4	$4(1-x)[-ln(1-x)]^{3/4}$	$[-ln(1-x)]^{1/4}$
Geometrical contraction models			
Contracting area	R2	$2(1-x)^{1/2}$	$[1-(1-x)^{1/2}]$

Contracting volume	R3	$3(1-x)^{2/3}$	$[1-(1-x)^{1/3}]$
Diffusion models			
1-D diffusion	D1	$1/2x$	$x^2$
2-D diffusion	D2	$[-\ln(1-x)]^{-1}$	$[(1-x)\ln(1-x)] + x$
3-D diffusion, Jander	D3	$3(1-x)^{2/3}/[2(1-(1-x))^{1/3}]$	$[1-(1-x)^{1/3}]^2$
Ginstling-Brounshtein	D4	$3/[2((1-x)^{-1/3}-1)]$	$1-(2x/3)-(1-x)^{2/3}$
Reaction-order models			
First-order	F1	$(1-x)$	$-\ln(1-x)$
Second-order	F2	$(1-x)^2$	$(1-x)^{-1}-1$
Third-order	F3	$(1-x)^3$	$[(1-x)^{-2}-1]/2$

### 3. Results and discussion

#### 3.1 Thermogravimetric analysis

Overall, changes in mass loss have paces that are not affected by the heating rate. Thus, we notice the first loss of mass of low intensity at the beginning of heating ( $T < 200^\circ\text{C}$ ), a loss of principal mass with strong intensity (for  $200^\circ\text{C} < T < 400^\circ\text{C}$ ) then for the strongest temperatures a low mass loss ( $T > 675\text{K}$ ). It thus seems at first sight that the decomposition of the red macroalgae under an inert atmosphere is done in 3 main stages taking place in the same temperature ranges, whatever the heating rates studied. However, under nitrogen, the derivative of the loss of mass as a function of time (hence the rate of loss of mass) shows a strong influence of the heating rate on the intensities of the mass-loss rates. Thus, the higher the heating rate, the greater the speed of loss of mass. In a second step, we note that the temperature corresponding to the maximum of the mass loss rate increases with the heating rate.

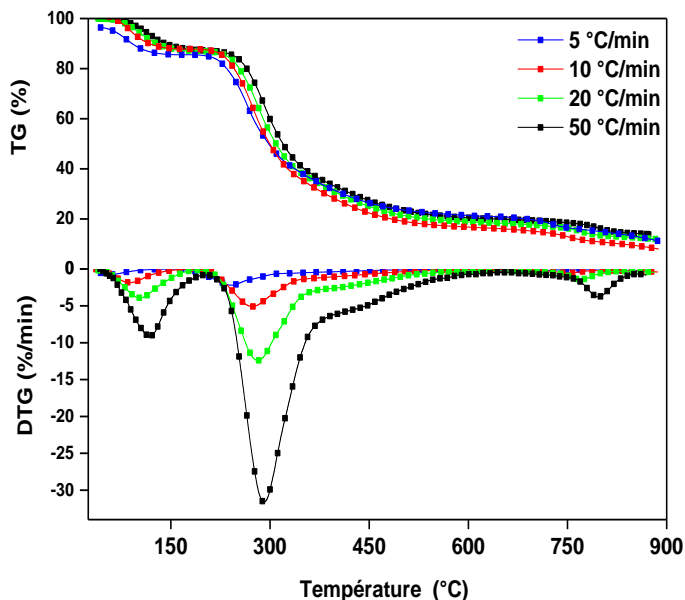


**Figure 1.** The TG and DTG curves of red algal at different heating rates.

The decomposition steps then observed for all the heating rates with changes in the intensities and the characteristic temperatures are as follows:

- A slight loss of mass up to the temperature of  $200^\circ\text{C}$  could be the drying of the samples during which residual moisture is removed.
- Between  $200^\circ\text{C}$  and  $400^\circ\text{C}$ , there is the largest loss in mass. In this temperature range, the degradation of red macroalgae is in one step. This step corresponds to the decomposition of the different biopolymers and can be attributed to the decomposition of carbohydrates and proteins. Similar studies were conducted for three samples of red macroalgae, [26] (*Pophyrayezoensis*, *Polcarniumtelfairiae* Harv, and *Corallinapilulifera*). *S. japonica* also exhibits similar degradation behaviors[27],
- Above  $400^\circ\text{C}$ , a slow mass loss is observed up to  $900^\circ\text{C}$ . This behavior corresponds to the slow process of residual carbon decomposition. A small proportion of inorganic materials in the ATG / DTG curves are decomposed at  $700\text{-}800^\circ\text{C}$ , probably due to carbonates [28]
- The heating rate is one of the most studied parameters during dynamic pyrolysis. This parameter often has a great influence on the thermograms representing the pyrolysis reaction. This influence is evident in the yield as well as the products obtained. Indeed, the products formed are partially destructible; and this destruction is even more important as the energy supplied to the system and when the pyrolysis is slow.
- From the curves TG in Figure III.1, we notice that when we vary the heating rate and keeping all the other factors constant, the end-of-reaction yield is about the same. Nevertheless, it has been shown that the heating rate has a strong influence on the nature of the products of the reaction for both the volatile matter and for the solid residue as well as on the kinetic parameters of the chemical reaction.
- (Radhakumari M et al 2016, Ceylan S et al 2014, Choi, JH et al 2017). Indeed, depending on the temperature of the reaction medium and the passage time in the reactor, the gaseous products that are released can degrade into small molecules of smaller sizes, polymerize or condense, and then attach to the solid residue. These fixed products are released when the temperature rises further. On the other hand, we observe thermograms to

the weather at low temperatures as the heating rate decreases. This phenomenon is very often observed in the literature [29]. This delay is caused by the energy supplied to the system which becomes more important when the heating rate decreases because even if the heat flow is low in the case of the small heating rates, the residence time is too high for that the sample stores enough energy to react quickly and break the chemical bonds that break when the energy of their formation is reached. This leads us to say that the pyrolysis of red macroalgae is a very sensitive reaction to the heating rate.

- Besides, changing the heating rate also causes a change in the DTG curves (Figure1). In addition to the shift in the thermogravimetric analysis case, we note that when we increase the healing rate, DTG peaks relating to the degradation rate become important. This could be explained by the fact that we are less likely to.

**3.2 Kinetic analysis**

The results obtained from thermogravimetric analysis were utilized to calculate the activation energy according to the differential and integral isoconversional methods. In this study, Friedman, FWO, and Vyazovkin methods were adopted to elaborate on the data. Firstly, the isoconversional Friedman method was employed to calculate activation energy from a plot of  $\ln\left(\frac{dx}{dt}\right)$  Friedman linear fit of a plot of

$\ln\left(\frac{dx}{dt}\right)$  against  $1/T$  for red algal thermal degradation process is shown in Table 2. The value of the activation energy was  $227 \pm 8$  kJ mol<sup>-1</sup> derived from the slope of such a regression line being  $-E_a/RT$ . Activation energies corresponding to the different conversion, have been also calculated using FWO and VYA methods according to Eqs. (8) and (10). The FWO plots of at progressing conversion values, with the slope of such line being  $1,052 \frac{E}{RT}$ , are displayed in Table 2. The Vyazovkin plots of  $\ln(\beta/T^2)$  versus  $1/T$  at progressing conversion values, with the slope of such line being  $-E_a/RT$ , are depicted in Table 2. The mean activation energies calculated from FWO and VYA methods were  $214 \pm 2$  and  $224,2 \pm 3$  kJ mol<sup>-1</sup> respectively. The dependence of apparent activation energy on the degree of conversion (x) ( $E_a-x$  curve) for the non-isothermal decomposition process of red algal obtained by isoconversional methods is presented in Fig. 2. From this figure, one can notice the same shapes of the curves  $E_a$  versus x corresponding to the considered isoconversional methods. Also, the values of apparent activation energy calculated by FWO and VYA integral methods are lower than the values of  $E_a$  calculated by FR differential method. The differences observed can be assigned to different approximations. It can be observed that the calculated average values of apparent activation energy for FWO and VYA methods are very similar.

**Table .3:** Calculation of  $E_x$  activation energies and  $R^2$  factor

méthode isoconversionnelle	Friedman		OFW		Vyazovkin	
	$E_x$	$R^2$	$E_x$	$R^2$	$E_x$	$R^2$
<b>x</b>						
<b>0.2</b>	238,30	0.9998	210,7	0.9908	217,71	0.9878
<b>0.25</b>	219,10	0.9943	211,53	0,9982	220,75	0,9985
<b>0.3</b>	218,90	0.9904	212,2	0,9917	221,46	0.9903
<b>0.35</b>	212,10	0.9988	215,77	0,9968	224,97	0,9973
<b>0.4</b>	218,00	0.9995	215,76	0,9968	224,88	0,9973
<b>0.45</b>	230,80	0.9998	213,16	0.9882	222,3	0.9855
<b>0.5</b>	230,80	0.9995	215,14	0,9932	224,09	0,9921
<b>0.55</b>	230,00	0.9998	215,14	0,9932	224,17	0,9915
<b>0.60</b>	230,80	0.9963	215,14	0,9932	224,77	0,9916
<b>0.65</b>	231,00	0.9935	215,14	0,9932	224,73	0,9917
<b>0.7</b>	231,30	0.9998	217,14	0,9963	228,28	0,9971
<b>0.75</b>	230,80	0.9995	217,14	0,9963	226,91	0,9972
<b>0.8</b>	231,80	0.9997	217,14	0,9963	226,98	0,997
<b>Valeur effective <math>E_x</math></b>	<b>227±8</b>		<b>214±2</b>		<b>224±3</b>	

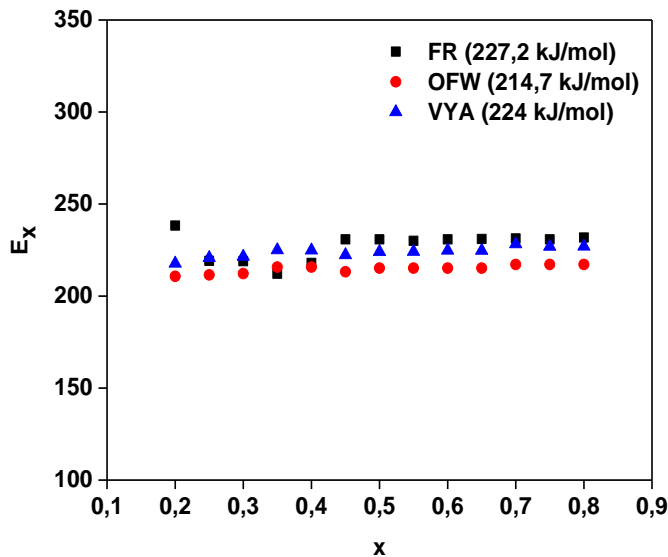


**Figure 2:** Variations of the activation energy  $E$  in the function of the conversion rate  $x$

The knowledge of  $x$  as a function of temperature and the value of the activation energy is essential to calculate the experimental masterplot against  $x$  from experimental data obtained under a linear heating rate (Eq. (14)). Fig. 3 shows the experimental master plots against  $x$  constructed from experimental data under Different heating rates using the 221.66 kJ mol<sup>-1</sup> mean activation energy obtained the FWO, VYA, and FR methods. The theoretical master plots corresponding to the  $g(x)$  functions in Table 2 are also shown in Fig. 3. It is shown that all experimental masterplots of the decomposition process at 5, 10, 20, and 50°C min<sup>-1</sup> are consistent with the theoretical master plot for F3 kinetic model. The comparison of the experimental masterplots with theoretical ones revealed that the kinetic process for the decomposition process of red algal was most probably described by Third-order (F3) model,  $g(x) = [(1 - x)^{-2} - 1]/2$

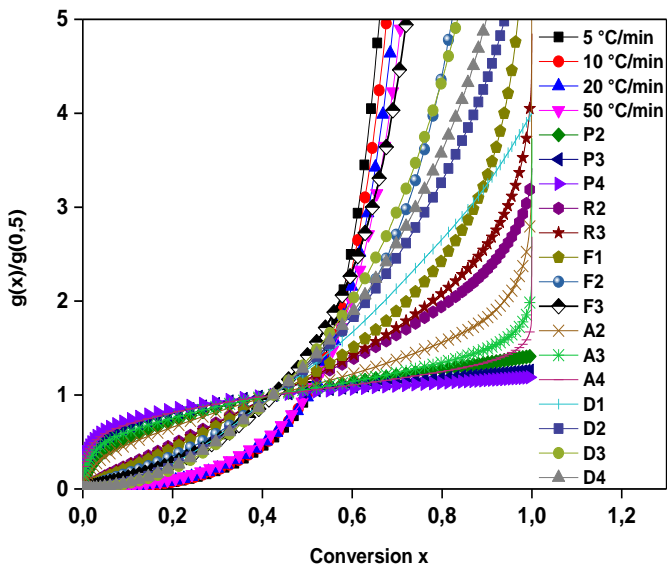


**Figure 3:** Kinetic curves (theoretical and experimental) using the method of Master Plots resulting from the integral form.

#### 4. Conclusions

This work explores the kinetics of the thermal degradation of red algae species *Gelidium* in a combined approach of is conversional and generalized master plot. The activation energy of the pyrolysis was between 214 and 227 kJ mol<sup>-1</sup> and it was found that a Reaction-order model F3). The kinetic model governs the reaction.

The results suggested that the experimental results and kinetic parameters provided useful information for the design of the pyrolysis processing system using algal waste as feedstock. Further investigation of pyrolysis products is required to fully understand the mechanisms of thermal degradation of redalgal.

#### References

1. J. M. Amezaga, D. Neil, and J. A. Hazelton, “ScienceDirect The future of bioenergy and rural development policies in Africa and Asia,” *Biomass and Bioenergy*, vol. 59, pp. 137–141, 2013.
2. O. K. Lee and E. Y. Lee, “Biomass and Bioenergy Sustainable production of bioethanol from renewable brown algae biomass,” *Biomass and Bioenergy*, vol. 92, pp. 70–75, 2016.
3. A. Aboulkas, A. Tabbal, H. Bouaik, M. El Achaby, K. El Harfi, and A. Barakat, “Thermochemical behaviour of Algal Waste: Kinetics and Mechanism of the Pyrolysis,” *Eng. Technol. J.*, 2018.
4. T. Ainane, “Valorisation de la biomasse algale du Maroc : Potentialités pharmacologiques et Applications environnementales , cas des algues brunes *Cystoseira tamariscifolia* et *Bifurcaria bifurcata* Tarik Ainane To cite this version : HAL Id : tel-00637002,” 2011.
5. N. Hanif, M. Chbani, and T. Naoki, “L ’ exploitation des algues rouges *Gelidium* dans la région d ’ El - Jadida : aspects socio-économiques et perspectives Abstract,” vol. 10, no. 1, pp. 103–126, 2014.
6. A. Mouradi-givernaud, L. A. Hassani, T. Givernaud, and Y. Lemoine, “Biology and agar composition of *Gelidium sesquipedale* harvested along the Atlantic coast of Morocco,” pp. 391–395, 1999.
7. F. Length, “Biotransformation of algal waste by biological fermentation,” vol. 5, no. July, pp. 1233–1237, 2006.
8. E. Fuente, R. R. Gil, and B. Ruiz, “Journal of Analytical and Applied Pyrolysis Pyrolysis characteristics of a macroalgae solid waste generated by the industrial production of Agar – Agar,” *J. Anal. Appl. Pyrolysis*, vol. 105, pp. 209–216, 2014.
9. E. Fuente and B. Ruiz, “Sustainable activated carbons of macroalgae waste from the Agar-Agar industry. Prospects as adsorbent for gas storage at high pressures,” *Chem. Eng. J.*, 2014.
10. M. V. Kok and E. Ozgur, “Energy Sources , Part A : Recovery , Utilization , and Characterization of lignocellulose biomass and model compounds by

- thermogravimetry,” *Energy Sources, Part A Recover. Util. Environ. Eff.*, vol. 39, no. 2, pp. 134–139, 2017.
11. G. MY *et al.*, “Utilization of Starink Approach and Avrami Theory to Evaluate the Kinetic Parameters of the Pyrolysis of Olive Mill Solid Waste and Olive Mill Wastewater,” *J. Adv. Chem. Eng.*, 2017.
  12. K. Wu *et al.*, “Bioresource Technology Pyrolysis characteristics and kinetics of aquatic biomass using thermogravimetric analyzer,” *Bioresour. Technol.*, vol. 163, pp. 18–25, 2014.
  13. H. Bouaik, A. Tabal, A. Aboulkas, K. El harfi, and C. A. Authors Aboulkas, “Investigation of the Pyrolysis Behaviour of Marine Macroalgae Biomass Using the Thermogravimetric Analysis,” *Eng. Technol. J.*, vol. 1, no. 09, pp. 2456–3358, 2018.
  14. A. Galadima and O. Muraza, “In situ fast pyrolysis of biomass with zeolite catalysts for bioaromatics/gasoline production: A review,” *Energy Conversion and Management*. 2015.
  15. A. Ounas, A. Aboulkas, K. El harfi, A. Bacaoui, and A. Yaacoubi, “Pyrolysis of olive residue and sugar cane bagasse: Non-isothermal thermogravimetric kinetic analysis,” *Bioresour. Technol.*, 2011.
  16. A. Aboulkas, K. El harfi, and A. El Bouadili, “Thermal degradation behaviors of polyethylene and polypropylene. Part I: Pyrolysis kinetics and mechanisms,” *Energy Convers. Manag.*, 2010.
  17. M. Y. Guida *et al.*, “Thermochemical treatment of olive mill solid waste and olive mill wastewater: Pyrolysis kinetics,” *J. Therm. Anal. Calorim.*, 2016.
  18. H. L. Friedman, “Kinetics of thermal degradation of char-forming plastics from thermogravimetry. Application to a phenolic plastic,” *J. Polym. Sci. Part C Polym. Symp.*, 2007.
  19. H. E. Kissinger, “Reaction Kinetics in Differential Thermal Analysis,” *Anal. Chem.*, vol. 29, no. 11, pp. 1702–1706, 1957.
  20. A. Aboulkas, A. Tabbal, H. Bouaik, M. El Achaby, K. El Harfi, and A. Barakat, “Thermochemical behaviour of Algal Waste: Kinetics and Mechanism of the Pyrolysis,” *Eng. Technol. J.*, vol. 3, no. 3, pp. 2456–3358, 2018.
  21. N. Sbirrazzuoli, “Determination of pre-exponential factors and of the mathematical functions  $f(\alpha)$  or  $G(\alpha)$  that describe the reaction mechanism in a model-free way,” *Thermochim. Acta*, vol. 564, pp. 59–69, 2013.
  22. A. Cadenato, J. M. Morancho, X. Fernández-Francos, J. M. Salla, and X. Ramis, “Comparative kinetic study of the non-isothermal thermal curing of bis-GMA/TEGDMA systems,” *J. Therm. Anal. Calorim.*, vol. 89, no. 1, pp. 233–244, 2007.
  23. A. Aboulkas *et al.*, “Investigation on the Pyrolysis Kinetics and Mechanism of Date Stone Using Thermogravimetric Analysis,” *Eng. Technol. J.*, vol. 3, no. 3, pp. 2456–3358, 2018.
  24. G. I. Senum and R. T. Yang, “Rational approximations of the integral of the Arrhenius function,” *J. Therm. Anal.*, vol. 11, no. 3, pp. 445–447, 1977.
  25. T. R. K. C. Doddapaneni, J. Kontinen, T. I. Hukka, and A. Moilanen, “Influence of torrefaction pretreatment on the pyrolysis of Eucalyptus clone: A study on kinetics, reaction mechanism and heat flow,” *Ind. Crops Prod.*, 2016.
  26. S. Kim, H. Vu, J. Kim, J. Hyung, and H. Chul, “Bioresource Technology Thermogravimetric characteristics and pyrolysis kinetics of Alga Sagarssum sp . biomass,” *Bioresour. Technol.*, vol. 139, pp. 242–248, 2013.
  27. R. K. Muktham and S. Bankupalli, “on ICTAC recommendations Pyrolysis characteristics and kinetics of algal biomass using tga analysis based on ICTAC recommendations,” no. January 2016, 2015.
  28. J. Hyung, S. Kim, H. Vu, J. Kim, and H. Chul, “Biomass and Bioenergy Effects of water-washing Saccharina japonica on fast pyrolysis in a bubbling fluidized-bed reactor,” *Biomass and Bioenergy*, vol. 98, pp. 112–123, 2017.
  29. S. Ceylan, Y. Topcu, and Z. Ceylan, “Bioresource Technology Thermal behaviour and kinetics of alga Polysiphonia elongata biomass during pyrolysis,” *Bioresour. Technol.*, vol. 171, pp. 193–198, 2014.